



**Electric fields in accelerating conductors:
Measurement of the EMF in rotationally accelerating coils**

Gareth F. Moorhead and Geoffrey I. Opat

School of Physics

The University of Melbourne

Parkville 3052, Victoria, Australia

(June 6, 1996)

Abstract

The acceleration of an electric conductor is predicted to produce an electric field proportional to m/q where m is the free mass and q the charge of the carriers of the electric current. In certain configurations this leads to a measurable EMF. In this paper we report a measurement of the EMF produced by rotationally accelerating coils of Aluminium and Copper wire. This experiment essentially repeats, using modern instrumentation, the 1916 Tolman - Stewart [1] experiment. The measured EMFs are found to agree with theory to better than 1%.

Typeset using REVTeX

I. INTRODUCTION

A. Motivation

In the 1960's Witteborn and Fairbank [2] attempted to determine whether positrons fell under gravity with the same acceleration as electrons. More recently there has been under development an experiment on the question of the fall of anti-protons versus protons under gravity [3]. These experiments necessitate an understanding of the state of electrification of their charged particle shielding systems which are also subject to the Earth's gravity.

After initial confusion it was realized that there are two effects of gravity in producing electric fields in conductors. One is the requirement that an electric field exists inside the material of the conductor to support the conduction electrons under gravity - the Schiff - Barnhill effect [4]. The other is the electric field which arises through the variation of the electron chemical potential in the solid due to the gravitationally induced strain gradient in the material - the "DMRT" effect [5]. This latter effect is larger than the first effect but does not give rise to an EMF which could drive electric current around a closed circuit. Both of these effects are of intrinsic interest, but for the purposes of the anti-matter fall experiments the theoretical predictions have been verified. The DMRT effect has been verified by Rossi [6], while a number of experiments have attempted to verify the Tolman - Stewart effect and hence the Schiff - Barnhill effect. These have been bedeviled by problems of noise and spurious pickup, especially at electrical contacts [7,8], which limited their precision. In this paper we report an experiment which is closer to the spirit of the original experiments of Tolman et al., one which is not so bedeviled by contact problems.

B. Previous experiments

While there have been a number of recent experiments conducted in response to the theoretical controversy which followed the predictions of Schiff and Barnhill [4], the earliest experiments of this type date back to the late nineteenth century. These early experiments

looked for mechanical effects in electrical phenomena, and vice versa, in attempts to understand the nature of electricity. Most well known are those of Maxwell which are described in his famous *Treatise on Electricity and Magnetism* [9]. Maxwell describes many experiments or possible experiments, including attempts to rotationally accelerate a coil of wire by rapidly changing the electric current (and hence the inertia associated with the charge carriers); attempts to cause precession of a "gyroscope" where the "rotor" was actually a coil conducting a current; and attempts to generate a pulse of electric current by rapidly accelerating or decelerating the spin of a coil of wire. The last of these experiments is similar to the one described here. All of these experiments were unsuccessful, the sensitivity required being beyond the technology of the day. However, very many of the theoretical issues, as well as experimental difficulties, were already well appreciated.

The measurement of the electric current or EMF induced by acceleration is generally regarded as having been successfully accomplished first by Tolman and co-workers. In 1916, Tolman and Stewart [1] reported measuring the pulse of electric current in a ballistic galvanometer connected in series with a rapidly spinning coil of wire when it was suddenly brought to rest. After many trials, and with great attention paid to the many experimental problems, values were reported for the ratio of mass to electric charge (compared with those of free electrons) of 1.11, 1.16 and 1.20 respectively for copper, aluminium and silver wire. These excesses were regarded as experimentally significant.

In order to improve precision, as well as to rectify some persistent systematic errors, the work was continued using a slightly different apparatus [10,11]. A solid copper cylinder was rotationally oscillated about its axis. The oscillating inertia induced electric current in the cylinder was detected by its magnetic coupling to a surrounding stationary coil of wire acting as secondary windings with the cylinder a single turn primary of a transformer. The use of an oscillating apparatus allowed detection with a tuned vibration galvanometer, while the motion was governed with elastic torsion rods. Again, great attention was paid to the very many spurious signals and other systematic errors. The averaged value of m/e of the 1923 experiment was 0.92 times theory, whereas that of the 1926 experiment was

0.81. The latter result included a measurement of a phase lag with respect to the motion of 10° . Although inconsistent with the earlier results, these results were again regarded as experimentally significant due to the extensive investigations of systematic errors.

Direct experiments on electron-inertia induced EMFs were not taken up again until more recent times. In the interval, however, several "inverse" electron inertia experiments were successfully pursued by Barnett [12] and others. In these experiments, the current in a coil of wire was altered with the accompanying change in angular momentum deduced from the macroscopic deflection of the suitably suspended coil. These results were in very close agreement with the free electron mass for a large variety of metals including those with positive Hall coefficients. Others [13,15,14] reported results close to unity for metals including Cu, Al, Cd, Zn and Mo. An advantage of these inverse experiments over the measurement of induced EMFs is their use of relatively coarse wire, greatly increasing the variety metals available for use.

More recently, several experiments have been motivated by the Schiff-Barnhill predictions, the Witteborn-Fairbank results and ensuing debate. Guptill [7] attempted to measure EMFs induced both by acceleration and by acceleration-induced strain with the same apparatus. These experiments were subject to spurious signals, giving results broadly in agreement with theory but with large uncertainties. A program of research aimed at clarifying experimentally the various electromagnetic effects in accelerated and stressed metals has been carried out at the University of Melbourne. Rossi [6] investigated electric fields just outside strained conductors, finding agreement with a more modern form of the DMRT theory. Darling [16] investigated the electric fields due to the different work functions of various crystal faces (the patch effect), finding considerable evidence for shielding by surface contaminants at all temperatures between 4K and 450K, even in ultra-high vacuum. In the area of electron-inertia induced EMFs, several [17-19] low (< 70 Hz) experiments were attempted using torsionally-accelerated coils and linearly-accelerated rods. These experiments did not measure a significant effect due to the very large spurious signals, mainly magnetic in origin. Davis [18] was able to measure an effect at ultra-sonic frequencies by inertially

generating electric standing waves in short rods of various metals. This work was considerably complicated by the appearance of thermo-electric EMFs due to the strain-induced thermo-elastic effect at ultra-sonic frequencies [8]. After taking this effect into account, the results for Ag, Al, Cu, Mo, Nb and Ti were all in reasonable agreement with theory.

II. THEORY

We discuss two approaches to the calculation of the EMF of a rotating coil.

Davis and Opat [8] show that the EMF, \mathcal{E} , induced in an accelerated conductor is given by the line integral

$$\mathcal{E} = \oint (m_e \mathbf{a} / e) \cdot d\mathbf{r} \quad (2.1)$$

where \mathbf{a} is the local acceleration of the conductor, and m_e and $-e$ are the mass and charge of the electron respectively ($e > 0$)¹. This expression was derived from the constitutive equation

$$\mathbf{I} = \sigma(\mathbf{E} + m_e \mathbf{a} / e + \nabla(\mu_e / e) - S \nabla \theta), \quad (2.2)$$

obtained by extending the usual constitutive equations to include acceleration [21]. In equation 2.2, \mathbf{I} is the current density, σ the conductivity, \mathbf{E} the electric field, μ_e the electrochemical potential of the free electron, S the Seebeck coefficient, and θ the absolute temperature.

In the case of the acceleration of a rigid body about a point \mathbf{r}_o , the acceleration of the point of the body at position \mathbf{r} fixed in the body measured from \mathbf{r}_o is given by

$$\mathbf{a} = \mathbf{a}_o + \dot{\boldsymbol{\Omega}} \times \mathbf{r} + \boldsymbol{\Omega} \times (\boldsymbol{\Omega} \times \mathbf{r}) \quad (2.3)$$

¹The sign convention is that the EMF will drive a conventional current in the direction of integration.

where \mathbf{a}_o is the acceleration of the point \mathbf{r}_o and $\Omega(t)$ is the (time dependent) angular velocity of the body. When this acceleration is used in equation 2.1, we find

$$\mathcal{E} = (2m_e/e)\dot{\Omega} \cdot \mathbf{S} \quad (2.4)$$

where \mathbf{S} is the vector area of the circuit. Note that equation 2.4 is analogous to the EMF, \mathcal{E}_m , induced by a uniform, but time-dependent, magnetic field $\mathbf{B}(t)$

$$\mathcal{E}_m = -\dot{\mathbf{B}} \cdot \mathbf{S}/c \quad (2.5)$$

where the velocity of light c should be omitted in SI units. We remark that in both cases the body in question may be a multi-turn coil of wire with external leads across which the EMF may be measured in principle with a high impedance voltmeter. Indeed, equation 2.5 provides a convenient way to determine \mathbf{S} experimentally which was used in the present work.

Whilst this theory applies to the present experiment, we present an alternative formulation of somewhat greater generality.

Consider the quantum mechanical Hamiltonian of a solid $H = H(\mathbf{p}_e, \mathbf{p}_n, \mathbf{r}_e, \mathbf{r}_n, t)$, where \mathbf{p}_e and \mathbf{r}_e are the momentum and position of the e -th electron, and \mathbf{p}_n and \mathbf{r}_n are the similar operators for the n -th nucleus. If the solid is now subject to an external electromagnetic field represented by the vector potential \mathbf{A} and scalar potential V , the Hamiltonian becomes, by virtue of the gauge-invariant coupling principle,

$$H' = H(\mathbf{p}_e + e\mathbf{A}, \mathbf{p}_n - Z_n e\mathbf{A}, \mathbf{r}_e, \mathbf{r}_n) - \sum_e eV + \sum_n Z_n eV \quad (2.6)$$

where $Z_n e$ is the charge on the n -th nucleus. If we have a changing magnetic field in a solenoid, the matter of which is described by this Hamiltonian, an EMF \mathcal{E}_m appears which arises solely from the electron momentum change in the Hamiltonian

$$\mathbf{p}_e \rightarrow \mathbf{p}_e + e\mathbf{A}/c. \quad (2.7)$$

The corresponding change to the nuclear momentum does not produce an EMF which can move electrons.

The EMF produced is given by the rate of change of magnetic flux

$$\mathcal{E} = -d\Phi_m/c dt \quad (2.8a)$$

where

$$\Phi_m = \int \mathbf{B} \cdot d\mathbf{S} = \oint \mathbf{A} \cdot d\mathbf{l} \quad (2.8b)$$

by Stokes' theorem, as $\mathbf{B} = \nabla \times \mathbf{A}$. If the magnetic field is uniform in space we may write

$$\mathbf{A} = \frac{1}{2} \mathbf{B}(t) \times \mathbf{r}. \quad (2.9)$$

We now consider a rotating system.

The quantum mechanics of a system in a frame of angular velocity $\Omega(t)$ about a fixed point is obtained by making the following changes respectively to the momentum and Hamiltonian

$$\mathbf{p}_e \rightarrow \mathbf{p}_e - m_e \Omega \times \mathbf{r}_e \quad (2.10a)$$

$$\mathbf{p}_n \rightarrow \mathbf{p}_n - m_n \Omega \times \mathbf{r}_n \quad (2.10b)$$

$$\begin{aligned} H(\mathbf{p}_e, \mathbf{p}_n, \mathbf{r}_e, \mathbf{r}_n, t) &\rightarrow H(\mathbf{p}_e - m_e \Omega \times \mathbf{r}_e, \mathbf{p}_n - m_n \Omega \times \mathbf{r}_n, \mathbf{r}_e, \mathbf{r}_n, t) \\ &\quad - 1/2m \sum_e (\Omega \times \mathbf{r}_e)^2 - 1/2 \sum_n m_n (\Omega \times \mathbf{r}_n)^2. \end{aligned} \quad (2.11)$$

With equation 2.9 substituted into equation 2.6 we see that $-2m_e c \Omega / e$ plays a role analogous to the magnetic field \mathbf{B} . Because of this analogy in the fundamental Hamiltonian of the system, and the theoretical prediction and experimental verification of equation 2.5 for the EMF in electromagnetic induction, we strongly expect the prediction of equation 2.4 to be verified.

The structure of this strong argument by analogy circumvents the need to include in the discussion the statistical mechanics and thermal physics of the system, the Pauli exclusion principle, and the specific quantum mechanics of electrons and holes. This is why we regard equation 2.4 as having high theoretical validity.

III. EXPERIMENTAL DESIGN

A. Apparatus

The expected inertially-induced voltage across the terminals of a coil of wire of equivalent area S executing rotary oscillations about its axis of amplitude θ_o at frequency f follows directly from Eqn. 2.4

$$V = kSf^2\theta_o \sin(2\pi ft + \phi) \quad (3.1)$$

where the constant k and the phase ϕ of the voltage relative to the rotary displacement are predicted to be

$$k = -4\pi^2 \left(\frac{2m_e}{e} \right) \approx 4.49 \times 10^{-10} \quad (3.2)$$

and

$$\phi \equiv \phi_V - \phi_\theta = 0. \quad (3.3)$$

In Eqn. 3.3, the phases ϕ_V of the voltage and ϕ_θ of the rotation displacement are both considered relative to the excitation phase for experimental convenience. In order to determine k and ϕ experimentally, the coil voltage amplitude V and phase ϕ_V , the rotation displacement amplitude θ and phase ϕ_θ , and the oscillation frequency f were all measured, with the coil area S measured separately by magnetic induction following Eqn. 2.5.

The main components of the apparatus were the coil to be rotated, a mechanical system to allow rotation and suppress other motions, an excitation system to supply the required rotational energy, an electrical system to measure the coil voltage, and a transducer to

measure the angular displacement. In experiments of this kind the signal sought is often very small compared with many signals which can arise accidentally in the apparatus. As an example, a coil with turns integrating to a total area S normal to the rotation axis of 1 m^2 , oscillating at 100 Hz with an amplitude of 1° develops an acceleration-induced EMF of only 8 nV amplitude. It is therefore necessary to optimize the mechanical and electrical design to minimize spurious signals and other errors. These include the angular displacement amplitude reading error, the spurious induction of EMFs in the coil by oscillating magnetic fields and by undesired motions of the coil in the residual magnetic field of the Earth, signals generated by triboelectric effects in the vibrating coil and signal leads, and the geometric effect of coil deformation. Lock-in amplifiers, which effectively suppress non-synchronous signals, were used to measure the voltage signals both across the sample coil and from the rotation transducer. Non-ferromagnetic materials were used wherever possible to reduce vibration-induced oscillating magnetic fields. Furthermore, use of metallic conductors of any sort was kept to a minimum to reduce oscillating magnetic fields arising from eddy currents induced by vibration.

The mechanical oscillator consisted of an elastic torsion bar oscillating near its first resonance (Fig. 1). The operation of this torsion bar near resonance had the advantages of nearly pure rotation about the axis as well as relatively large angular acceleration. The torsion bars developed for the project featured an 'X' shaped cross-section machined from circular rods of the non-ferromagnetic metals Phosphor-Bronze or Beryllium-Copper, or of plastic. The main advantage of the 'X' section was its much greater flexural stiffness for a given torsional stiffness compared with circular, annular or other cross-sections. In combination with the coil design this allowed troublesome flexural modes to be pushed to much higher frequencies than the torsional modes. Furthermore, by choosing an appropriate thickness of the cross vanes, the torsional stiffness could be readily matched with the coil moment of inertia to select operating frequencies. The end sections by which the bar was clamped and the central section on which the coil was mounted were kept circular and of slightly larger diameter to ensure good mechanical coupling and to minimize deformation and

frictional losses. The torsional resonator, consisting of bar and coil, was mounted in a rigid, open aluminium frame clamped to a massive non-magnetic support structure. The rotational motion was excited by two parallel linear electromagnetic drive units operating in balanced anti-phase to produce a pure couple. These drive units were clamped to a massive slate slab and well shielded magnetically with an inner rigidly coupled concentric copper tubes and outer uncoupled concentric copper tubes. Particular care was taken with the magnetic shielding of the drive units because they generate strong magnetic signals oscillating at the same frequency as the coil and thus evading rejection by the lock-in amplifier. The inner shields attenuated the field arising from the AC drive-coil current, whereas the outer shields attenuated the oscillating field arising from the residual mechanical vibration of the strong permanent magnets. Long rods between the drive and torsion bar also allowed the sensitive coil to be placed at a large distance, approximately 3 m. Spurious signals at the sample coil were measured using stationary coils positioned near the rotating sample coil and in the sample coil with the drive shafts disconnected. The drive shafts themselves were stiff perspex tubes lightly coated in graphite spray to eliminate triboelectric charging in the atmosphere. A computer-controlled function generator provided a common excitation signal to the two lock-in amplifiers and, via an optical fibre, to the well-shielded high power audio amplifiers which provided the drive currents.

The sample coils were wound from thin insulated copper or aluminium wire using a machine devised for the purpose, each layer being set in epoxy resin to ensure rigidity and to facilitate production of high winding densities. In order to maximize the number of turns and hence coil area for a given moment of inertia, the wires were as thin as could be successfully wound without breaking, typically 120 μm diameter. The electrical Johnson noise arising from the higher resistance of thinner, longer wires was negligible after lock-in amplification with all coils having a resistance of less than 1 k Ω . Sample coil shapes were generally intermediate between the extremes of long and narrow, and thin and wide, in order to less flexibility and have a higher moment of inertia which would act to reduce the frequencies of flexural modes. Coils were typically 10 mm high, 10 mm thick and with outer radii from 20

to 70 mm. Sixteen coils with integrated areas ranging from approximately 1 to 6 m² were used for the main investigation. Oscillation frequencies ranged from approximately 100 to 800 Hz, maximum rotation amplitudes were typically between 0.1° and 1° and maximum expected signal amplitudes were typically between 1 and 2 μ V.

It proved very difficult to arrange signal leads from the vibrating coil to the stationary preamplifier input without generating significant spurious signals from microphonic and thermoelectric effects. Initial attempts using low-noise, thin coaxial cable mounted as close to the centre of the coil - where displacement was minimum - were unsuccessful due to residual microphonic induction of synchronous pickup. The system finally devised consisted of four stages. Short lengths of an uninsulated copper-alloy wire (resistant to metal fatigue) were soldered to the two ends of the coil wire and wrapped several times around the coil in the same direction. These parallel leads came tangentially away from the coil in a parallel loop which also provided some strain relief. Their ends were soldered to copper rods protruding from a relatively massive copper tube into which the rods had been potted with epoxy. This tube, which was clamped to a massive, vibration-isolated lead block, acted as a mechanical vibration filter. Beyond the tube the signal was carried by a shielded, twisted-pair cable of a design found to have very low microphonicity. The two signal leads finally ended in separate lengths of coaxial cable leading to the differential inputs of the preamplifier.

The expectation of a signal synchronous with the mechanical excitation of the system led naturally to the choice of lock-in amplifiers for electrical measurements.

The use of phase-sensitive detection by lock-in amplifiers lead to efficient rejection of asynchronous signals. Care was nevertheless taken to ensure that the total signal including asynchronous pickup remained within the linear operating range of the amplifier chain, and that the small fraction of noise present in the narrow lock-in passband remained negligible. Two lock-ins of the same model [22] were used, one for the sample signal and one for a rotation displacement transducer. Since measurement of the relative phases of the two signals was required, the in-phase and quadrature components were recorded alternately. The same instrument also provided for accurate frequency measurement. Control and data

acquisition was accomplished over an IEEE-488 bus connecting a personal computer, the two lock-in amplifiers and the function generator providing the fundamental excitation.

Many of the serious interfering signals arose from interaction of the ambient constant magnetic field with the vibrating sample coil and through secondary oscillating magnetic fields generated by eddy currents in vibrating metal components. In order to render these effects negligible, care was taken to reduce greatly both the field strength and field gradients, since both act to induce currents in vibrating conductors via their angular and linear displacements respectively. The apparatus was located in a large room where it was sited away from iron furniture and building framework such that the static field was relatively 'flat'. The coil and support structures were surrounded by three orthogonal sets of large diameter Helmholtz coils for independent reduction of field components. The field was monitored with sensitive ring-core flux-gate magnetometers allowing field levels across tens of centimetres to be reduced to less than 10^{-7} T. The Helmholtz coils also permitted the application of strong static and oscillating magnetic fields for diagnostic purposes and for the measurement of the integrated coil area S . By using a uniform, accurately calculable coaxial oscillating magnetic field, coil area could be measured in situ using the same detection system as the main experiments, thus eliminating several potential systematic errors.

Rotation amplitude was measured with a transducer based on passage of light through semi-crossed polarisers. One piece of polariser projected from the periphery of the moving coil while another was fixed nearby. Unlike many other kinds of displacement transducer, this type of system is largely immune to effects of linear displacement or orthogonal rotation. Use of optical fibres to deliver and capture light removed a source of synchronous interference. The light signal detected by a photodiode was measured with a lock-in amplifier of the same model used for signal measurement with the similar harmonic responses. Since in effect the two measurements are used in a ratio, a number of potential systematic errors were thus eliminated.

IV. RESULTS

In a typical experimental run, the excitation frequency was scanned across the resonance while the average in-phase and quadrature components of the sample coil voltage and the rotation transducer signals were alternately recorded, and their amplitudes and relative phase calculated. Data from one such scan are plotted in Fig. 2, while the same data adjusted using the separately measured rotation amplitude and coil integrated area to a reference amplitude and area are plotted in Fig. 3. The effect of the varying amplitudes on the error estimates can be seen, as can the expected parabolic behaviour with frequency. For convenience in analysis, frequency is treated as a dependent variable since it is both subject to the least experimental uncertainty and the parameter against which greater than linear variation was expected.

Many such runs were performed over a frequency ranges from less than 100 Hz to about 800 Hz, using a number of coils fabricated with either Copper or Aluminium wire. A selection of these runs is summarized, again adjusted using the separately measured rotation amplitude and integrated coil area, in Fig. 4. The data sets were analyzed by fitting the expected quadratic frequency dependence to the signal amplitude, and the expected zero constant value to the phase. Consistency checks were performed by variously permitting constant and linear terms in the amplitude fit. The error estimates at all stages were believed dominated by systematic errors and spurious signals, rather than being statistically random. Results are presented in Table I. Each incorporated point includes a separate measurement of voltage amplitude and phase, rotation amplitude and phase, frequency and integrated coil area, as well as the assumption that the mass to charge ratio of the charge carriers is that of the free electron, m_e/e .

V. CONCLUSION

The EMFs induced by rotational acceleration in coils of Copper and Aluminium wire have been measured and found to agree with the theoretical prediction to within the error estimates. These results contradict the historic results of Tolman et al. [1,10,11] where discrepancies of 10 - 20 % were observed, and improve on more recent results [7,8,16]. Further details may be found in [23].

TABLES

TABLE I. Results summarized for the two different metals tested. The amplitude result is presented as a ratio of the measured and expected quadratic coefficient k of Eqn. 3.2, whereas the phase is the difference between the voltage and rotation phases relative to the excitation phase as in Eqn. 3.3. Error estimates are dominated by estimates for residual systematic errors and spurious pickup.

Metal	Amplitude (Meas./Theor.)	Phase
Copper	0.997 ± 0.012	$-0.7^\circ \pm 0.9^\circ$
Aluminium	0.994 ± 0.012	$-0.5^\circ \pm 0.9^\circ$

ACKNOWLEDGMENTS

We acknowledge the support of the Australian Research Council.

REFERENCES

- [1] R. C. Tolman and T. D. Stewart, *Phys. Rev.* **8** 97 (1916)
- [2] F. C. Witteborn and W. M. Fairbank, *Phys. Rev. Lett.* **19** 1049 (1967)
- [3] R. E. Brown, J. B. Camp and T. W. Darling,
Eleventh Accelerator Conference, Denton, Texas (1990)
- [4] L. I. Schiff and M. V. Barnhill, *Phys. Rev.* **151** 1067 (1966)
- [5] A. J. Dessler et al., *Phys. Rev.* **168** 737 (1968)
- [6] F. Rossi and G. I. Opat, *J. Phys. D: Appl. Phys.* **45** 11249 (1992)
- [7] E. W. Guptill, *Can. J. Phys.*, **49** 3150 (1971)
- [8] T. J. Davis and G. I. Opat, *Class. Quantum Grav.* **5** 1011 (1988)
- [9] J. C. Maxwell, *A Treatise on Electricity and Magnetism* Clarendon Press (1891);
reprinted Dover Publications (1954)
- [10] R. C. Tolman et al., *Phys. Rev.* **21** 525 (1923)
- [11] R. C. Tolman and L. M. Mott-Smith, *Phys. Rev.* **28** 794 (1926)
- [12] S. J. Barnett, *Rev. Mod. Phys.* **7**, 129 (1935)
- [13] C. F. Kettering and G. C. Scott, *Phys. Rev.* **66** 257 (1944)
- [14] S. Brown and S. J. Barnett, *Phys. Rev.* **87** 601 (1952)
- [15] G. C. Scott, *Phys. Rev.* **8** 542 (1951)
- [16] T. W. Darling, F. Rossi, G. I. Opat and G. F. Moorhead, *Rev. Mod. Phys.* **64** 237
(1992)
- [17] J. Brody, M.Sc. thesis, The University of Melbourne (1982)
- [18] T. J. Davis, Ph. D. thesis, The University of Melbourne (1987)

- [19] A. A. Verheijen, Ph. D. thesis, Rijksuniversiteit te Leiden (1992)
- [20] G. I. Opat, Aust. J. Phys. **46** 647 (1993)
- [21] S. R. De Groot and P. Mezur, *Non-Equilibrium Thermodynamics*, North Holland, Amsterdam (1962)
- [22] Model SR510 Single-phase Lock-in Amplifier,
Stanford Research Systems, Sunnyvale, California, USA.
- [23] G. F. Moorhead, Ph. D. thesis, The University of Melbourne (1992)

FIGURES

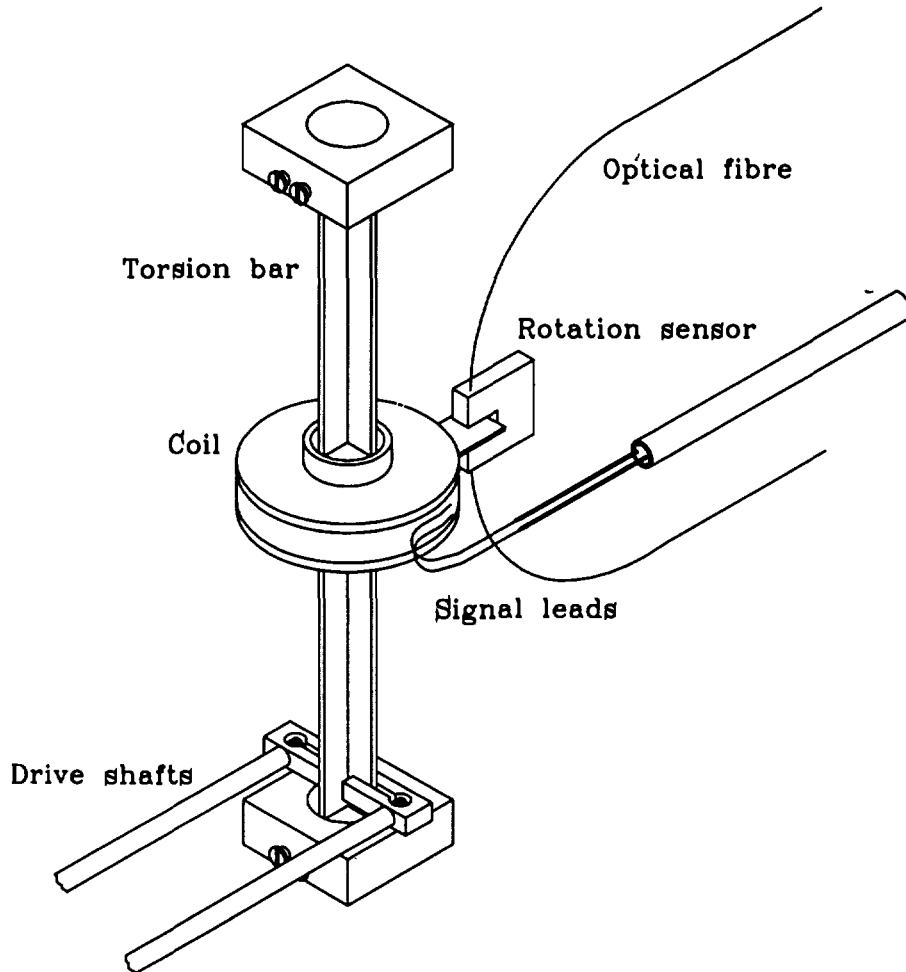


FIG. 1. Sketch of the test coil and torsion bar. Note the cross-shaped cross-section of the bar, chosen to separate flexural and torsional vibration modes by making the bar much stiffer in bending than in torsion. Excitation was provided by two push-rods vibrating in anti-phase. Note shown are rigid frame and massive support structure on which the assembly was mounted, nor the vibration-isolated three-axis set of Helmholtz coils to eliminate the constant geomagnetic field.

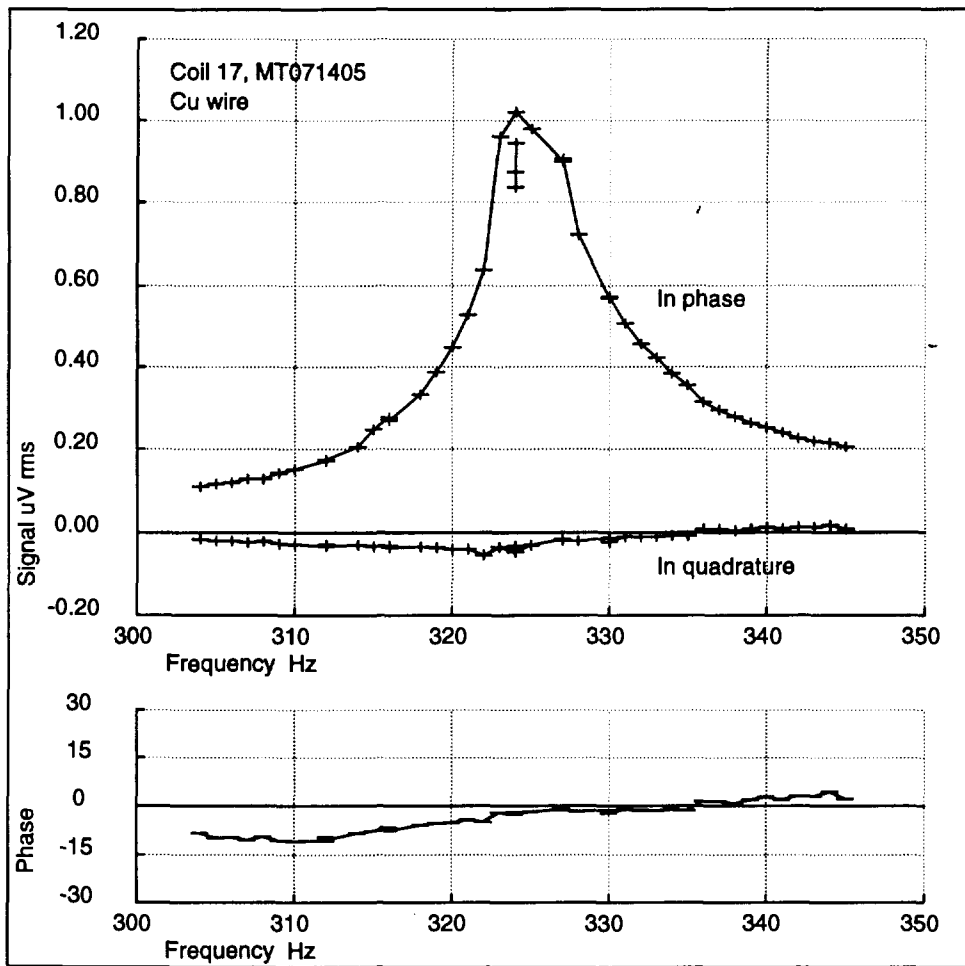


FIG. 2. Coil voltage amplitude and phase data from a typical experimental run. The solid line connects theoretically predicted values.

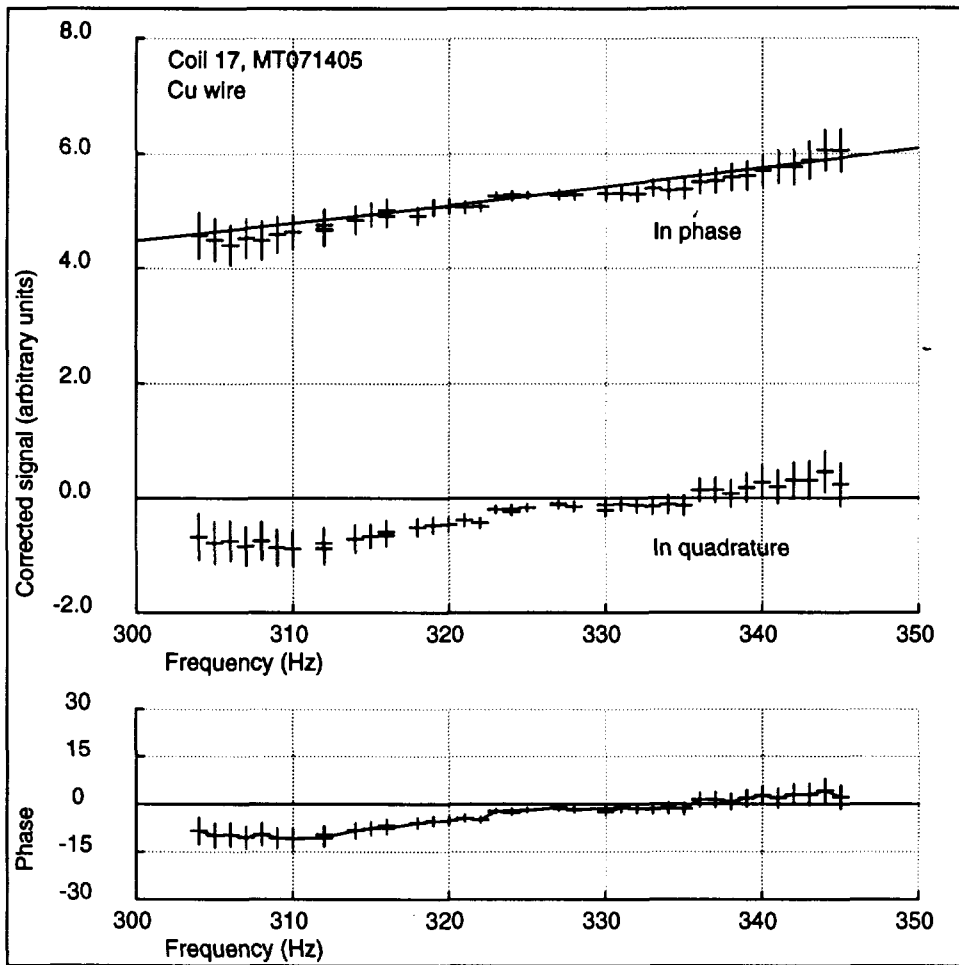


FIG. 3. The same data as the experimental run of the previous figure adjusted for rotation amplitude to a common reference value using the rotation transducer measurements. The solid line shows the theoretically predicted signal parabolic with frequency.

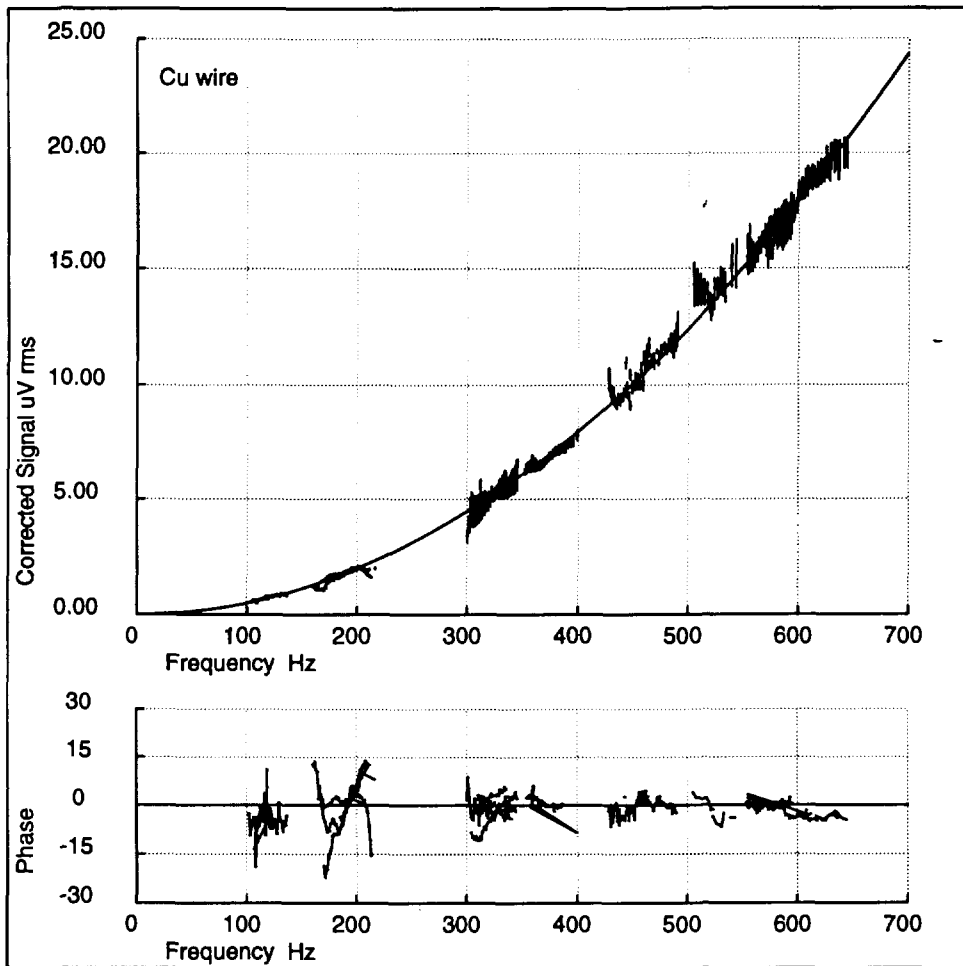


FIG. 4. Summary of Copper data corrected for separately measured rotation amplitude and coil areas plotted against frequency to show the expected quadratic behaviour. The solid lines represent the theoretical predictions. Similar results were obtained for Aluminium.